Contribution to the 9th International Colloquium on Atomic Spectra and Oscillator Strengths for Astrophysical and Laboratory Plasmas, Lund*, Sweden - August 7-10, 2007, published in Physica Scripta* T134, 014026 (2009)

Spectroscopy of highly-charged tungsten ions relevant to fusion plasmas

C Biedermann[1], R Radtke[1], R Seidel[1], and T Pütterich[2]

[1]Institut für Physik der Humboldt-Universität zu Berlin, Lehrstuhl Plasmaphysik, Newtonstr 15, 12489 Berlin, and Max-Planck-Institut für Plasmaphysik, EURATOM Association, 17491 Greifswald, Germany

[2]Max-Planck-Institut für Plasmaphysik, EURATOM Association, 85748 Garching, Germany

E-mail: Christoph.Biedermann@ipp.mpg.de

Abstract. The Berlin EBIT has been established by the Max-Planck-Institut für Plasmaphysik to generate atomic physics data in support of research in the field of controlled nuclear fusion by measuring the radiation from highly charged ions, particularly tungsten ions, in the x-ray, extreme ultraviolet and visible spectral ranges. With EBIT a selected ensemble of ions in specific charge states can be produced, stored and excited for spectroscopic investigations. Employing this technique, we have investigated the soft x-ray lines at 0.56 nm from Cu-like W^{45+} to V-like W^{50+} ions originating from $3d$-$4f$ transitions, which are also observed in the high-temperature core plasma of the ASDEX Upgrade tokamak. A further study focuses on Si-like W^{60+} to Ne-like W^{64+} tungsten ions predicted to dominate the core plasma of ITER and radiate strongly at 0.13 nm from n=3-2 transitions.

1. Introduction

The need for spectroscopic information on radiation from tungsten ions has been pushed by the intensified use of tungsten as plasma facing material in present-day experimental fusion devices like ASDEX Upgrade, JET and the currently, at Cadarache, France, being constructed International Thermonuclear Experimental Reactor (ITER) [1]. With the substantial progress in performance and knowledge of magnetically confined fusion plasmas achieved during the last decade ITER will prove its option as primary energy source in the future. ITER's objective is to demonstrate the scientific and technological feasibility of controlled nuclear fusion power generation, integrate and test all essential fusion power technologies and components and show safe and environmental acceptable operation [2,3]. In order for the plasma facing components to withstand the high particle and power load produced by particles escaping the magnetic confinement, tungsten is projected as wall material of choice due to its favorable properties. The high energy threshold of sputtering, the low sputtering yield, the high redeposition efficiency, the low tritium retention and the excellent thermal properties as compared to low-Z materials like carbon and Be make it a candidate to armor future fusion reactors. Employing tungsten as shield for the first wall will nevertheless introduce W as intrinsic impurity to the plasma. Already in 1970s, the thread of W radiation produced by not-completely-stripped ions of

minor W concentrations in the plasma preventing burning in a fusion reactor was realized at the ORMAK [4]. However, nowadays divertor configurations used in tokamaks and scenarios of magnetic confinement allow good separation of the hot bulk plasma from the plasma-facing wall and reduce strongly the erosion. To investigate this issue ASDEX Upgrade is refurbished with complete tungsten-covered plasma-facing components for the current measurement campaign [1]. If tungsten penetrates into the central plasma, it will not be fully stripped. At the electron temperatures of 10 to 25 keV in the core plasma for ITER conditions the partly-ionized W raises tremendously the power loss by emission of line radiation. This poses a serious problem for the energy confinement possibly quenching fusion reactions and setting a limit on the relative tungsten concentration to a few times 10^{-5} in the core. Careful control of the tungsten impurity is a prerequisite for future fusion devices.

Accurate atomic physics data is needed, including information on atomic transitions with wavelengths, line intensities, and cross sections for ionization, excitation and recombination for a large range of charge states of tungsten ions, in order to develop diagnostics measuring tungsten concentrations in fusion plasmas und provide support for modeling predictions.

Spectroscopic information at fusion devices is deduced from measurements integrating the radiation along the line-of-sight reaching through the plasma of the fusion device. In this case, emission may originate from regions with different excitation conditions given by the radial profile of electron temperature and density. The strong influence of plasma transport processes and the occurrence of a large number of ionization states emitting simultaneously further complicates data interpretation and identification [4-7]. Recently applied high-Z accumulation technique restricts the number of emitting ionization states [8], however the data analysis needs additional support by plasma modeling.

In figure 1 (right) an example illustrates the expected fractional abundance of tungsten charge states for conditions prevailing at ASDEX Upgrade and ITER, with a central electron temperature of 4 resp. 18 keV and assuming a tungsten concentration of 10^{-5}. This shows the wide range of simultaneously radiating ionization states across the normalized radius of the machine (ρ_{pol}). In the left part of figure 1 a synthetic spectrum resulting from STRAHL calculations using atomic data of the Cowan code is plotted [9]. This gives an overview of the wavelength range of lines emitted by the color-marked range of tungsten charge states. The figure points out that certain ionization states at certain wavelength intervals may serve as diagnostic for certain plasma regions. For ITER conditions, the expected charge state distribution spans from Ag-like W^{27+} at the outer edge of the plasma up to F-like W^{65+} in the hot core requiring sophisticated and specialized detection and analysis systems for line identification.

With a much smaller experimental device, namely the electron beam ion trap (EBIT), a well-selected ensemble of ions in specific charge states can be produced, excited and confined for extended periods of detailed spectroscopic observation [10-12]. EBIT employs a mono-energetic electron beam to successively ionize atoms up to a selected charge state controlled by the energy of the electron beam, excite and trap the ions within the beam's space charge potential. This technique has the advantage over experiments on tokamak plasmas that the ions charge state distribution is restricted to only a few states depending on the atom's ionization potential versus the acceleration potential of the electron beam. The EBIT electron densities of $3 \cdot 10^{12}$ cm^{-3} ensure that electron excitation processes similar to fusion plasmas dominate radiative transitions and with the mono-energetic beam energy no integration over a range of electron temperatures and densities occurs.

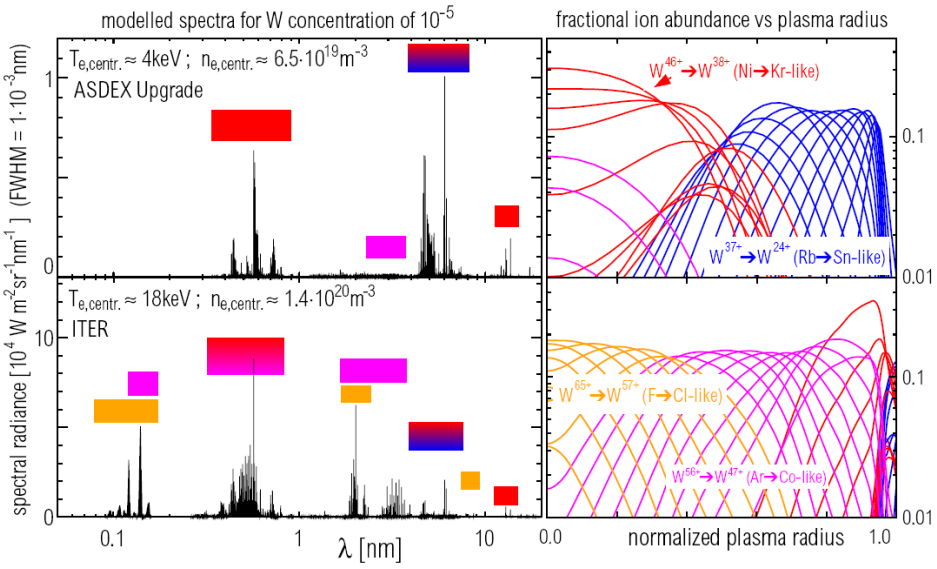

Figure 1: Predicted tungsten line spectrum and charge state distribution in ASDEX Upgrade and ITER plasma for a central electron temperature of 4, respectively 18 keV and a tungsten concentration of 10^{-5}. The coloured bars in the spectra (left) mark the emitting charge states (right).

2. Experiment

The experiments presented here used the Berlin EBIT to produce and excite highly charged tungsten ions and analyse the emitted radiation [10]. The main component of EBIT is the electron beam extracted from a heated cathode inside the electron gun and accelerated in several steps to the 3-sectioned drift tube assembly floating at high potential. This potential defines the electron beam energy. For an electron beam current of 50 mA the beam-energy spread is limited to about 30 eV FWHM. The drift tubes are surrounded by a pair of Helmholtz-coils providing a 3-tesla magnetic field, which compresses the electron beam to a diameter of 70 µm in the 4-cm-long region of the drift tubes. By biasing the two end-drift-tubes positively with respect to the middle segment, an axial trap is formed. The strongly compressed electron beam produces a space-charge potential-well confining the ions in radial direction and additionally enhances the collision rate between electrons and injected atoms and ions in the trapping region successively ionizing the trapped specie to higher charge states. Further, the electron beam serves to excite the ions. Tungsten is introduced to the trap as tungstenhexacarbonyl evaporated from a powder into a differentially pumped gas injector.

The radiation emitted by the ions trapped in EBIT is analyzed by high resolution x-ray and EUV spectroscopy [13]. A flat-crystal Bragg spectrometer equipped with a large area ADP-crystal and a position sensitive detector is used to study x-ray lines in the wavelength range from 0.04 to 1.6 nm with a resolution of about $\lambda/\Delta\lambda \approx 1000$. Extreme-ultraviolet emission diagnostics from 3 to 100 nm was accomplished by means of a 2 m Schwob-Fraenkel grazing-incidence spectrometer operating with $\lambda/\Delta\lambda \approx$ 200-4000. All the spectral measurements are calibrated *in situ* by recording hydrogen- or helium-like reference lines with wavelengths known accurately from standard data base. Auxiliary, a window-less solid-state ultra-low energy germanium detector is applied to monitor the x-radiation between 0.4 and 30 keV energy (corresponding to 31 and 0.4 nm in wavelength values) with large solid-angle and high detection efficiency resulting in broad-band spectra of the ion inventory of EBIT.

By stepping the electron beam energy in small increments the charge state distribution of trapped ions is limited to a particular value by the ionization potential of the specie. Following the variation of spectral features across a range of beam energies and ionization thresholds reveals which lines can be

attributed to particular charge states. Line identification is supported by comparison with theoretical predictions.

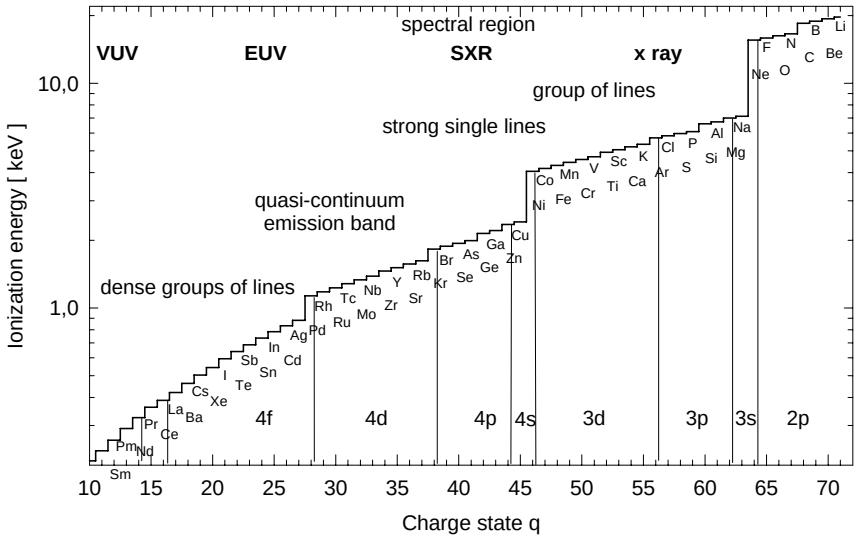

Figure 2. Ionization energies of highly charged tungsten ions and overview of spectral emission features.

3. Tungsten radiation

Once tungsten erodes from surfaces and penetrates the high temperature plasma of fusion devices a plentitude of tungsten ion-charge states may be produced across the confined plasma profile due to the Maxwell distribution of electron energies. This is exemplified in figure 1 for a plasma in ASDEX Upgrades and in ITER presenting the tungsten ion abundance along the cross section of the device. While for ASDEX Upgrade Ni-like W^{46+} to Kr-like W^{38+} ions can be expected in the central, respectively Rb-like W^{37+} to Sn-like W^{24+} at the outer plasma region, the distribution of these ion stages will be squeezed at ITER to the outer edge, and F-like W^{65+} to Cl-like W^{57+} will dominate the central high-temperature region and Ar-like W^{56+} to Co-like W^{47+} ions appear further outwards of the core. In figure 2 the specific signatures and dominant wavelength ranges of observed tungsten emission lines are marked in a plot showing the stepwise increase of the energy required to ionize a certain charge state. This overview sections the involved outer shell-configurations for each charge state with labels of the isolectronic sequence.

Tungsten spectroscopy started at the ORMAK tokamak with the observation of an unresolved, wide, band-like emission structure around 5 nm [4] which was further confirmed with investigations at ASDEX Upgrade [7]. Later EBIT studies at Berlin [10] and Livermore [14] monitored the lines of many charge states contributing to this signature. At the Berlin EBIT the structure was identified with the help of HULLAC calculations and a collisional-radiative model. The multiplicity of densely spaced lines due to many different ionization stages of tungsten form a quasi-continuum emission band originating from *4p-4d* and *4d-4f* transitions of ion states with open *4d* subshells with strong configuration mixing. The wide structure thereby formed was labeled unresolved transition array. The sequence of EUV-CCD-images for EBIT beam energies between 0.8 and 1.7 keV presented in Ref. [10], shows a the quasi-band line-emission pattern which shifts progressively from 5.1 to 5.3 nm with tungsten ion states increasing from Rh-like W^{29+} up to Rb-like W^{37+}. Calculations with the HULLAC package showed the importance of mixed configurations and the need to employ a collisional-radiative model to explain the narrowing of the emission band with respect to statistical-weight modeled spectra.

Many of the same ions (W^{29+}-$^{37+}$) for which strong electric dipole transitions around 5 nm are observed, emit also magnetic dipole radiation around 70 nm. The lines appear well isolated in a limited wavelength interval which makes them particular suitable for monitoring [13]. For each ion charge state, a few distinct single lines are observed and identified as originating from transitions between $4p^6 4d^n$ *(n=1-9)* ground-term fine structure levels. Certain intensity ratios of M1-lines to resonant E1 lines of particular ion states show a strong dependence on the electron density, or respectively the electron temperature and are therefore well suited as plasma diagnostic.

Moving on to the hotter central plasma regions at ASDEX Upgrade or towards the edge of the main plasma column at ITER it is predicted that tungsten is ionized to Zn-like W^{44+} up to Cr-like W^{50+}. As figure 1 shows the most prominent line radiation of these ion charge states is located in the soft-x-ray spectral region around 0.5 nm. We have investigated the radiation in the wavelength interval 0.50 to 0.62 nm using a vacuum flat-crystal spectrometer. Figure 3 summarizes in a set of plots the spectra for electron beam energies between 3.03 and 4.69 keV. The measured line intensities vary as function of the beam energy and enhance considerably when the population of the emitting ion within EBIT is at maximum. For beam energies 3.03 and 4.12 keV, the most abundant tungsten ions in the trap are Cu-like W^{45+} and Ni-like W^{46+}. The dominant tungsten line at 0.5685±5 nm is assigned to a $3d^{10} - 3d^9 4f$ transition in Ni-like W^{46+}. At the 3.03-keV beam-energy spectrum a line at 0.5747 nm signifies a minor contribution of Zn-like W^{44+}. As the beam energy progressively increases, the ion population in the EBIT shifts to higher charge states. For the sequence following the 4.12-keV spectrum, the observed weakening of the 0.5685-nm Ni-like W line indicates the extinction of W^{46+} ions for beam energies above 4.2 keV. If the electron beam energy is increased further, we produce and excite successively Co-like W^{47+}, Fe-like W^{48+}, Mn-like W^{49+} and finally at 4.69 keV Cr-like W^{50+} giving rise to a multitude of lines observed in the narrow wavelength range 0.5 to 0.62 nm shown in the spectra of figure 3. The line features from these ions incorporate contributions from a large number of *3d-4f* transitions, since they are wider than expected for a single line. Additionally to the measured spectra, figure 3 displays in the upper panel of each spectra-plot a calculated spectrum for each single charge

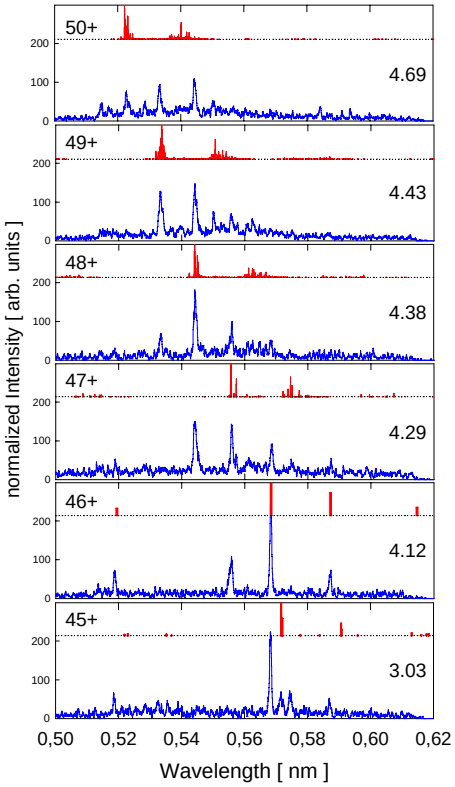

Figure 3: Comparison of measured and predicted soft x-ray spectra of tungsten. Experimental data (blue line) are labelled (right) with the electron beam energy in units [keV] applied to EBIT. The calculated data (red histogram) plotted above the observed spectra are marked with the charge state (left) and are taken from Ref. [15].

state. The simulated spectra are generated by *ab initio* calculations using the HULLAC-package and relative populations for each level are obtained from collisional-radiative modeling [15]. From the comparison of the experimental and theoretical spectra shown in figure 3 it is evident that the observations confirm the general pattern, intensity relation and line position within each spectrum. Similar studies of M-shell spectra of tungsten ions conducted at the Lawrence Livermore National Laboratory EBIT confirm the identifications [16].

Looking at even hotter plasma regions like the central plasma of ITER, it is envisaged that electron temperatures of $T_{e,centr}$=18 keV are reached. For these plasma conditions, tungsten is predicted to be ionized to Cl-like W^{57+} and up to F-like W^{65+} charge states in the core region (figure 1). Tungsten ions of this ionization degree have an open or empty n=3 shell and when excited emit strong lines from n=3-2 transitions. This L-shell radiation produces lines around 0.13 nm as marked with a yellow bar in the lower spectrum of figure 1. At the Berlin EBIT we have started to investigate ions of these charge states and their radiation.

Setting for example the electron beam energy of EBIT to 15 keV, tungsten ions up to Ne-like W^{64+} are produced. The energy required to ionize to the next higher charge state is 15.566 keV, limiting the charge state distribution to W^{64+}. The wide range x-ray spectrum observed with a Ge-solid-state detector presented in figure 4 is dominated by the *n=3-2* radiation emitted from these ions, showing up in four line structures at 8.3, 9.1, 9.6 and 10.4 keV x-ray energy. Further, higher shell transitions (*n=4-2*) as well as transitions to *n=3* from direct excitation to higher *n* are registered. All these emission lines emerge from a background of bremsstrahlung, which decreases with increasing x-ray energy and ceases at the energy equivalent to the electron beam energy. One special feature of EBIT is the fact that the signature of the radiative recombination (RR) process appears in the x-ray spectrum as distinct lines. The x-ray energy is well defined by the narrow electron-beam energy distribution (typically, FWHM 50 eV) and the binding energy of the capture state of the recombining ion. With increasing radiative capture level, the binding energy decreases and the RR-structure merges towards the value equivalent to the electron beam energy. Figure 4 shows the x-ray spectrum of highly charged tungsten produced with 15 keV electron beam energy. The intensity distribution of radiative recombination to the *n=3* level is highlighted and displayed in detail to the right in figure 4(b). We have exploited the information of the RR-intensity distribution to gain knowledge about the charge state abundance trapped and excited in EBIT. For each ion charge state the energy of recombination to each n=3 subshell (angular momentum state) is determined and the RR-line is widened by the electron beam distribution folded with the detector response. The theoretical RR intensity is calculated from

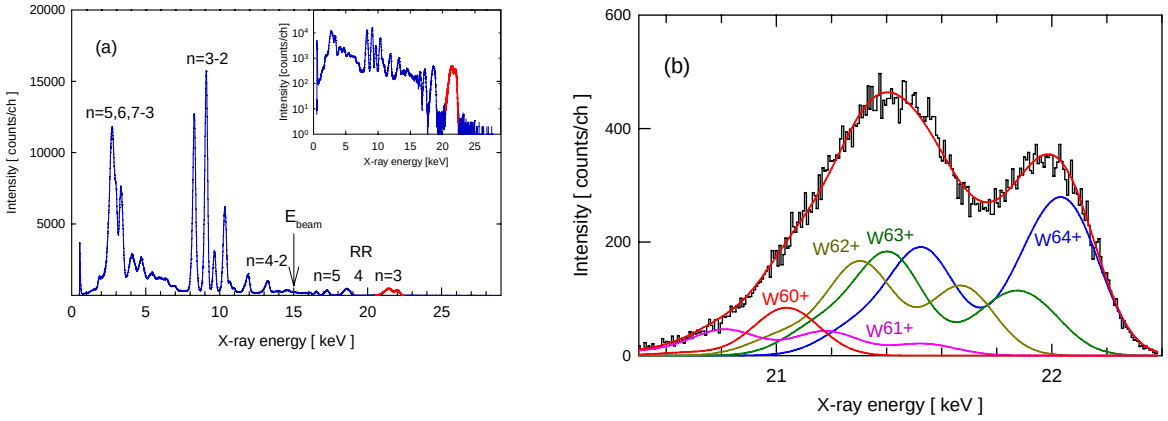

Figure 4: (a) Wide range x-ray spectrum of tungsten produced in the EBIT at 15.0 keV electron beam energy and 120 mA electron current. The inset shows the x-ray spectrum with a logarithmic intensity scale to emphasize the RR contribution. **(b)** Enlarged detail of the radiative recombination to *n=3*. Intensities are given in counts per channel.

the well-known RR cross section, the electron beam properties, geometry and detection efficiency. A fit of the theoretical distribution for all relevant ion states to the experimental RR-spectrum yields the charge state abundance. For the RR-spectrum shown in figure 4(b) the resulting charge state distribution is presented in figure 5(b).

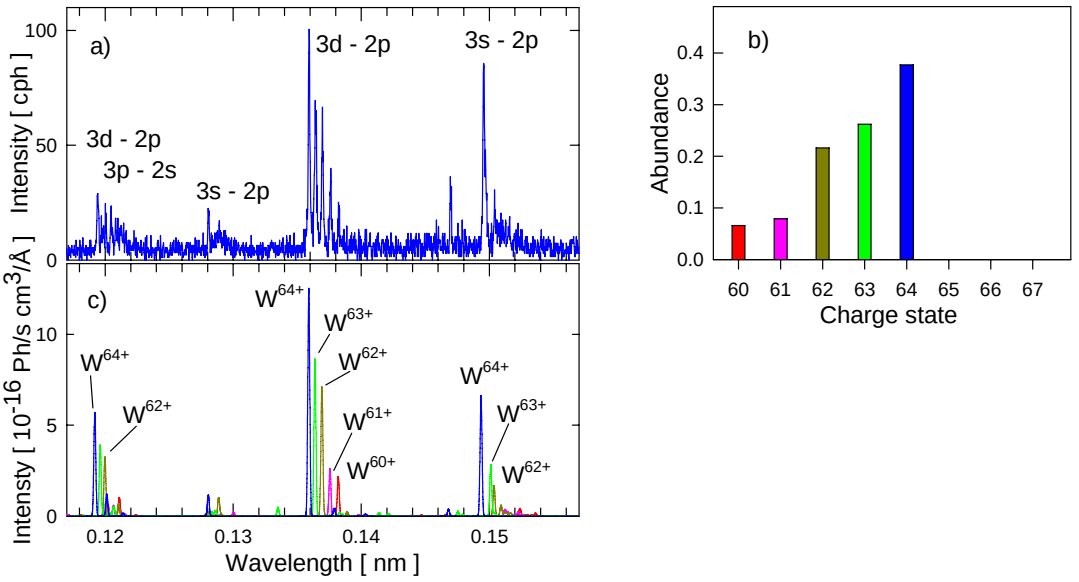

Figure 5: L-shell spectra of tungsten. (a) Bragg-crystal spectrum observed at EBIT with 15.0 keV electron beam energy and 120 mA electron current. Intensity is given in counts per channel and hour. (b) Histogram of the corresponding charge state abundance and (c) predicted intensity distribution.

The dominant x-ray structures emitted from these tungsten ions (W^{64+} to W^{60+}) origins from n=3-2 transitions and are analyzed in further detail with the flat-crystal spectrometer. The resulting spectrum is presented in figure 5 and shows how each of the four structures observed with lower resolution as one line splits into a sequence of lines from different ion charge states attributed to groups of 3*p*-2*s*, 3*d*-2*p* and 3*s*-2*p* transitions and a weaker line group of 3*s*-2*p* transitions at 0.128 nm. The graph of figure 5(a) is assembled from two spectrometer settings due to the limited wavelength-range accepted by the detector and the narrow rocking curve of the LiF (220) crystal. Identification of the lines has been supported by calculations using the computer codes from the ADAS project [17] which include atomic structure calculations using the Cowan-code and serve as input for a collisional radiative model. Further, the ion abundance extracted from the analysis of the radiative recombination measurement enters the calculations. Some of the theoretical lines are very closely spaced and are folded with a 0.00025nm-FWHM Gaussian to resemble detector resolution. The wavelengths values have been corrected by fully relativistic atomic structure calculations of GRASP [18]. The predicted x-ray intensity distribution shown in figure 5(c) demonstrates that each line within a group corresponds to transitions of a particular ion charge state. To the lower wavelength side each of the transition group (n=3*p*-2*s*, 3*d*-2*p*, 3*s*-2*p*) is headed by a line produced by the dominant Ne-like W^{64+} ion. Lines from transitions of the next lower charge state ions are shifted slightly to larger wavelength values. Overall, the calculated intensity distribution agrees well with the measured spectrum. One difference is the W^{64+} line measured at 0.1468 nm with larger intensity than theory predicts for the $2p^5\ 3p\ ^3D_2 - 2p^6\ ^1S_0$ electric quadrupole transition. This type of analysis has been performed for L-shell spectra at electron beam energies between E_e=9.5 and 20.6 keV to investigate the line intensity distribution as function of

the ion charge state abundance in EBIT. The extracted information may help to interpret the spectra observed at the tokamak.

References

[1] Neu R, 2006 *Phys. Scr.* **T123** 33
[2] Aymar R, Barabaschi P, and Shimonmura Y, 2002 *Plasma Phys. Control. Fusion* **44** 519
[3] Skinner C, *this volume*
[4] Isler R C, Neidigh R V and Cowan R D 1977 *Phys. Lett.* **A66** 295
[5] Hinnov E, Mattioli M 1978 *Phys. Lett.* **66A** 109
[6] Finkenthal M, Huang L K, Lippmann S, Moos H W, Mandelbaum P, Schwob J L, Klapisch M, and the Text Group 1988 *Phys. Lett.* **A127** 255
[7] Assmusen K, Fournier K B, Laming J M, Neu R, Seely J F, Dux R, Engelhardt W, Fuchs J C, and the ASDEX Upgrade Team 1998 *Nucl. Fusion* **38** 967
[8] Pütterich T, Neu R, Biedermann C, Radtke R, and ASDEX Upgrade Team 2005 *J. Phys. B: At. Mol. Opt. Phys.* **38** 3071
[9] Pütterich T, Neu R, Dux R, Whitheford AD, O`Mullane MG, and the ASDEX Upgrade Team 2008 *Plasma Phys. Control. Fusion* in press
[10] Radtke R, Biedermann C, Schwob J L, Mandelbaum P, and Doron R 2001 *Phys. Rev.* **A64** 012720
[11] Utter S B, Beiersdorfer P, and Träbert E 2002 *Can. J. Phys.* **80** 1503
[12] Ralchenko Yu, Reader J, Pomeroy J M, Tan J N and Gillaspy J D 2007 *J. Phys. B: At. Mol. Opt. Phys.* **40** 3861
[13] Radtke R, Biedermann C, Fussmann G, Schwob J L, Mandelbaum P, Doron R 2007 *IAEA Atomic and Plasma-Material Interaction Data for Fusion* **13** 45
[14] Utter S B, Beiersdorfer P and Träbert E 2002 *Can J Phys* **80** 1503
[15] Fournier K, 1998 *At. Data Nucl. Data Tables* **68** 1 and private communication
[16] Neill P, Harris C, Safranova A S, Hamasha S, Hansen S, Safranova U I , and Beiersdorfer P 2004 *Can J Phys* **82** 931
[17] Summers H P, 2004 *The ADAS User Manual, version 2.6* http://adas.phys.strath.ac.uk
[18] Grant I P, Johnson C T, Parpia F A and Plummer E P 1989 *Comput. Phys. Commun.* **55** 415